Published in final edited form as:

Cancer Res. 2016 October 01; 76(19): 5777–5787. doi:10.1158/0008-5472.CAN-15-2936.

miR-1298 inhibits mutant KRAS-driven tumor growth by repressing FAK and LAMB3

Ying Zhou[1], **Jason Dang**[1,2], **Kung-Yen Chang**[1,2], **Edwin Yau**[3,4], **Pedro Aza-Blanc**[1], **Jorge Moscat**[5], and **Tariq M. Rana**[1,2,4,6]

[1]Program for RNA Biology, Sanford Burnham Prebys Medical Discovery Institute, La Jolla, CA 92037

[2]Department of Pediatrics, University of California San Diego, 9500 Gilman Drive MC 0762, La Jolla, California 92093

[3]Division of Hematology-Oncology, Department of Internal Medicine, University of California San Diego, La Jolla, CA 92037

[4]Solid Tumor Therapeutics Program, Moores Cancer Center, University of California, San Diego, 3855 Health Sciences Drive, La Jolla, CA 92093

[5]Cancer Metabolism and Signaling Networks Program, Sanford Burnham Prebys Medical Discovery Institute, La Jolla, CA 92037

[4]Institute for Genomic Medicine, University of California San Diego, 9500 Gilman Drive MC 0762, La Jolla, California 92093

Abstract

Global microRNA functional screens can offer a strategy to identify synthetic lethal interactions in cancer cells that might be exploited therapeutically. In this study, we applied this strategy to identify novel gene interactions in KRAS mutant cancer cells. In this manner, we discovered miR-1298, a novel miRNA that inhibited the growth of KRAS-driven cells both in vitro and in vivo. Using miR-TRAP affinity purification technology, we identified the tyrosine kinase FAK and the laminin subunit LAMB3 as functional targets of miR-1298. Silencing of FAK or LAMB3 recapitulated the synthetic lethal effects of miR-1298 expression in KRAS-driven cancer cells, whereas co-expression of both proteins was critical to rescue miR-1298-induced cell death. Expression of LAMB3 but not FAK was upregulated by mutant KRAS. In clinical specimens, elevated LAMB3 expression correlated with poorer survival in lung cancer patients with an oncogenic KRAS gene signature, suggesting a novel candidate biomarker in this disease setting. Our results define a novel regulatory pathway in KRAS-driven cancers which offers a potential therapeutic target for their eradication

Correspondence: trana@ucsd.edu.

Conflict of Interest: The authors declare no competing financial interests.

INTRODUCTION

Mutations in the KRAS oncogene are found in approximately 20% of human cancers and is the most commonly mutated gene in the RAS family of oncogenes (85% of RAS mutations are KRAS mutations). RAS is a GTPase that cycles between GTP-bound (active) state and GDP-bound (inactive) forms through the actions of guanine nucleotide exchange factors (GEFs) and GTPase-activating proteins (GAPs). Activating mutations found in cancers (most commonly at conserved codons 12 and 13) impair the GTPase activity of KRAS, resulting in the constitutive activation of KRAS and its downstream pathways, including the RAF-MEK-MAPK and PI3K-AKT pathways that regulate critical cell processes such as proliferation and survival (1,2). Activating KRAS mutations are major driver mutations in non-small cell lung cancer (NSCLC) with mutations in KRAS found in about 30% of NSCLC cases, representing the largest fraction of known driver mutation associated NSCLC. KRAS mutations are also frequently identified in 40–50% of colorectal cancers (CRC), and KRAS mutational status is a key factor in deciding on treatment options for metastatic CRC patients due to the ineffectiveness of anti-EGFR antibody (cetuximab or panitumumab) therapy in metastatic CRC patients with mutant KRAS (2). In NSCLC, KRAS mutations are generally mutually exclusive to both EGFR mutations and ALK rearrangements, and KRAS mutated cancers are generally resistant to targeted tyrosine kinase inhibitors targeting these driver mutations (erlotinib for EGFR mutations and crizotinib for ALK rearrangements).

Despite decades of effort, no targeted therapy is yet available clinically for KRAS mutated cancers despite much effort. Due to the absence of well-defined binding pockets at key active sites (3), efforts to inhibit KRAS activity with small molecules have been largely fruitless (4–6). For this reason, synthetic lethal approaches, in which genetic perturbations or drugs that are normally not lethal to the cell become lethal in the presence of another genetic perturbation (in this case KRAS oncogenic mutation), have been utilized to identify potentially tractable targets for therapy. Several groups have conducted systematic RNA interference (7–11) or small molecule (12) screens to identify synthetic lethal interactions with oncogenic KRAS. Such screens have identified novel targets such as PLK1, TBK1, STK33, and GATA2.

Prior functional genomic screens have largely focused on coding genes. Although more than 90% of the human genome is transcribed, only ~ 2% codes for proteins (13), highlighting the importance of noncoding RNAs for biological function. Non-coding RNAs (ncRNA) are now implicated as crucial regulators of diverse aspects of cellular processes. Among the different ncRNAs, small conserved sequences called microRNAs (miRNA) have been the best characterized over the past decade and are known to be involved in crucial cellular processes and widely dysregulated in cancer. MicroRNAs (miRNAs) are small (~22 nucleotide) noncoding RNAs that regulate gene expression post-transcriptionally by binding to specific regions in the 3′UTR of mRNA targets to promote their degradation and/or inhibit their translation. Because a single miRNA can potentially bind to and regulate hundreds, even thousands, of targets, they can have profound effects on gene expression networks (14). Accordingly, numerous miRNAs have been shown to regulate vital cellular processes in both physiological and pathological conditions (15).

miRNAs are generally downregulated in tumors (16) with many miRNAs acting as tumor suppressors. Impairment of miRNA maturation has been reported to enhance the transformed phenotype of cancer cells and accelerate tumor formation in KRAS-driven models of lung cancer (17). The well studied let-7 family of miRNAs were the first miRNAs to be implicated with RAS (18) and have been shown to repress KRAS expression and inhibit mutant KRAS dependent cancer cell growth in vitro and tumor growth in vivo (18–20). Other miRNAs have been implicated as KRAS tumor suppressors, miRNA-96 in KRAS pancreatic cancer (21), miRNA-181a in KRAS mutant oral squamous cell carcinoma (22), and miRNA-30b in CRC (23).

In this study, we screened a library of human miRNA mimics to identify novel synthetic lethal interactions with oncogenic KRAS mutation. In screening for synthetic lethal interactions, two main approaches have been traditionally utilized: screening across large panels of different cell lines harboring different mutations or comparing paired isogenic cell lines which are derived from identical parental cell lines but differ in the mutation of interest. We used both approaches in the current study, carrying out an initial screen in an isogenic colorectal cell line differing only in the presence or absence of an activating KRAS mutation, and then validating our hits in a panel of lung cancer cell lines with and without KRAS mutations. By combining cell lineages from both CRC and NSCLC with different KRAS activating mutations, we sought to identify more conserved synthetically lethal KRAS interactions with potentially less lineage dependence. Utilizing this approach, we identified miR-1298 and its targets, FAK and LAMB3, as suppressors of KRAS-dependent cell growth in both CRC and NSCLC contexts, and demonstrate that ncRNAs can be used for synthetic lethal screens to functionally annotate their function and uncover novel signaling regulatory pathways in cancer.

MATERIALS AND METHODS

Cell lines and cell culture

The paired isogenic HCT116 $KRAS^{WT/-}$ and HCT116 $KRAS^{WT/G13D}$ colon cancer cell lines were kind gifts from Dr. Bert Vogelstein (Johns Hopkins, Baltimore, MD). A549, NCI-358, NCI-H460, NCI-H522, NCI-H1568, NCI-H1792, NCI-H23, NCI-H1975, and NCI-H1437 were obtained from the ATCC (Manassas, VA). HCT116 cells were cultured in DMEM (Invitrogen) with 10% FBS (Invitrogen) and 1% Pen/Strep (Invitrogen). All lung cancer cell lines were cultured in RPMI 1640 (Gibco) with 10% FBS and 1% Pen/Strep. HCT116 Cell lines were validated by PCR amplification and Sanger Sequencing to confirm the mutation at the genomic level. Strict bio-banking procedures were followed and cells were tested for contamination, including mycoplasma. All other cell lines were obtained from ATCC and used within 2–4 months.

Transfection of miRNA mimics and siRNA

Cells were transfected with miRNA mimics or siRNAs by reverse transfection using RNAiMAX (Invitrogen), according to the manufacturer’s recommendations. siRNAs were used as pools of 4 per gene (Dharmacon SMARTpools) unless specified. For the miRNA mimic library screening, the HCT116 isogenic pair (800 cells/well in 384-well plates) were

reverse transfected with 10 nM of a human miRNA mimic library containing ~858 mimics (Ambion) and 0.1 μL RNAiMax/well. Cell lines were used 5 days post-transfection.

Cell viability and proliferation

Cells were plated in triplicate at 3000 cells/well in 384- or 96-well plates. Five days later, cell viability was determined using the ATPLite luminescent assay (PerkinElmer) according to the manufacturer's instructions. Luminescence signals were normalized and the average of triplicates was designated the cell viability score. A viability score of 1.0 indicates no difference between test cells and cells treated with a control miRNA mimic. For validation, proliferation was also measured with CyQUANT NF Cell Proliferation Assay Kit (Invitrogen), which uses a fluorescent cell-permeable DNA-binding dye.

Lentivirus production and infection

Lentiviruses were produced by transfection of 293T cells with pMIF-Zeo-cGFP-miR-1298 or pMIF-Zeo-cGFP-miR-Ctrl vectors (construction described below) together with the packaging plasmids FIV and VSV-G using Fugene HD (Roche). Culture supernatants containing lentiviruses were collected at 48 h and 72 h after transfection. Viral supernatants were pooled and stored at −80°C. NSCLC cells were infected with a 1:10 dilution of supernatant in polybrene-containing medium. Cells were selected with zeocin starting at 24 h after infection. After 72 h, 80%–90% of the cells were GFP+.

Xenograft mouse model

NSCLC cells were infected with miR-Ctrl- or miR-1298-expressing lentiviruses for 72 h, washed, and resuspended. Groups of 6 Balb/c nude mice were injected subcutaneously into the left and right flanks with 10^6 control or miR-1298-infected cells. Tumor dimensions were measured with calipers for up to 40 days, and volumes (mm^3) were calculated as (0.5 × width) × ($height^2$).

Western blot analyses

Cells were lysed in RIPA buffer. Protein samples were resolved by SDS-PAGE and then subjected to western blot analysis with anti-LAMB3 (kindly provided by Dr. M. Peter Marinkovich), anti-actin (Sigma), or anti-FAK (Cell Signaling) antibodies.

TUNEL staining

NCI-H460 cells and NCI-H522 cells were transfected with miR-Ctrl or miR-1298 mimics, cultured for 5 days, and then fixed with 10% paraformaldehyde. TUNEL (Terminal deoxynucleotidyl transferase-mediated deoxyuridine triphosphate (dUTP) nick-end labeling) staining was performed using a TUNEL kit (Roche). Nuclei were counter-stained with 4′,6-diamidino-2-phenylindole (DAPI). The cells were imaged using a Leica DM13000 immunofluorescent microscope, and TUNEL+ cells were enumerated using the software.

Prediction of miRNA targets

Putative miR-1298-binding sites were identified with rna22 and TargetScan (http://www.targetscan.org) pattern-based algorithms. rna22 (https://cm.jefferson.edu/data-tools-

downloads/rna22-v2-0/) generates full-length target sites; that is, each predicted heteroduplex extends beyond the corresponding miRNA seed region.

Luciferase assays

HeLa cells were seeded at 1×10^5 cells/well in 12-well plates 24 h before transfection. miR-1298 or miR-Ctrl mimics were co-transfected at a final concentration of 25 nM with 200 ng of the psiCHECK-2 vector. This vector constitutively expresses firefly luciferase, allowing transfection efficiency to be controlled. Forty-eight hours after transfection, firefly and *Renilla* luciferase activities were measured consecutively with the dual-luciferase reporter system (Promega). All luciferase assays were repeated a minimum of 3 times, each with biological duplicates.

RNA extraction and quantitative PCR

For quantitative PCR analyses, total RNA was extracted from cells using TRIzol reagent (Invitrogen) according to the manufacturer's instructions. cDNA synthesis was performed with 500 ng of total RNA and Superscript II, according to the manufacturer's instructions (Bio-Rad). PCR was performed using SYBR Green PCR Master Mix with *GAPDH* as an internal control. Primer sequences were designed by the Roche Universal Probe Library and are available on request. All amplicons were analyzed using a Roche LightCycler 480 II.

Vector construction

The mammalian expression vectors for LAMB3 and FAK were purchased from Open Biosystem (Colorado). $KRAS^{G12V}$ in a pCMV-Myc vector was a gift from Dr. Huaxi Xu. cDNAs encoding LAMB3 and FAK were subcloned using pcDNA4.0.

pMIF-cGFP-Zeo vector (SBI), a FIV-based microRNA precursor construct, was used to express miR-1298. The construct consists of the miR-1298 stem-loop structure and 220 bp of upstream and downstream flanking genomic sequences. The mature miR-1298 sequence can be obtained from http://www.mirbase.org/.

psiCHECK-2 vector (Promega) was used for the luciferase assay. For LAMB3-MREs, the sequence corresponding to the rna22-predicted miRNA-MRE (or mutated sequence for LAMB3-MRE-MUT; Figure S4E) were synthesized as sense and antisense oligomers, then annealed and cloned into psiCHECK-2 directly downstream of *Renilla* luciferase. For FAK, the full 3′ UTR was cloned into psiCHECK-2. The mutant construct was generated by PCR-directed mutagenesis using a primer pair containing the mutant MRE sequence. The PCR product was subsequently used as a template for full-length PCR.

Foci formation assay

H460 cells or H1437 cells in a 10 cm dish were transfected with 30 nM miR-1298 mimic or miR-Ctrl mimic. After 12 h, the cells were reseeded into 6-well plates in DMEM plus 10% FBS and incubated for 2 weeks. The cells were then fixed with formalin, stained with 0.5% crystal violet, and the colonies were counted.

miR-TRAP technology

miRNA mimics were chemically modified at 2 distinct positions in the antisense/guide strand of miR-1298, as previously described (25). Briefly, psoralen (Pso) was covalently attached to the 2′ position of the sugar ring of a uridine within the miRNA-1298 seed sequence (position 5 from the 5′ end), and a biotin was conjugated to the 3′ end for affinity purification. To ensure a high yield of Pso-modified miRNAs, the coupling reaction was conducted using an excess molar ratio of activated Pso to amine-containing miRNA mimics (2′O protected, Dharmacon) in DMSO in the presence of N,N-diisopropylethylamine in the dark. After 24 h, excess Pso was removed by precipitating the modified miRNAs with ethyl acetate, and the Pso-functionalized miRNA mimics were analyzed by UV spectroscopy and denaturing PAGE. Subsequent analysis of deprotected single-stranded RNAs by denaturing gel electrophoresis clearly showed single bands with slower electrophoretic mobility compared to the unmodified strand, confirming that the miRNAs were efficiently conjugated to Pso.

For crosslinking experiments, HCT116 cells were seeded in 15 cm dishes at a density of 2×10^6 cells/dish. HCT116 were transfected with 25 nM of the miR-1298-TRAP probe using Lipofectamine 2000 (Invitrogen), according to the manufacturer's protocol. Twenty-four hours later, the culture medium was removed and cells were rinsed 3 times with PBS, 10 ml of PBS was added, and the cells were irradiated for 5 min with UVA (360 nm) in a photochemical reactor (Rayonet, model RPR-100) equipped with 16 RPR-3500 light tubes. Cells were then lysed by addition of 3 ml lysis buffer (20 mM Tris, pH 7.5, 200 mM NaCl, 2.5 mM $MgCl_2$, 0.5% NP-40, and 80 U RNaseOUT) and shaken on a rocker at 4°C for 5 min. Cells were collected by scraping the plates, and cell debris was removed by centrifugation at 13,000 rpm at 4°C for 15 min. The supernatant was removed and ~1 ml was mixed with streptavidin-conjugated Dynabeads M-280 (Invitrogen) and rotated at 4°C for 4 h. The tubes were placed on a magnet for 2 min, the supernatant was removed, and the beads were washed with 3 times with 500 μl lysis buffer for 5 min each. TRIzol reagent (200 μl) was added to the bead sample and RNA was extracted according to the manufacturer′s protocol. Final RNA samples were suspended in 7.5 μl RNase-free water and reverse transcribed using Superscript II (Invitrogen). qPCR was performed using a Roche LightCycler 480 II and SYBR Green master mix (Bio-Rad). qPCR primers were designed by Roche Universal Probe Library, and sequences are available upon request.

Survival analysis

Associations between LAMB3, LAMA3, and LAMC2 expression and NSCLC patient survival were based on a published study (27) of gene expression data and survival outcomes from a large cohort of lung cancer patients. Statistical analysis of gene expression and prognosis of patients carrying $KRAS^{MUT}$ versus $KRAS^{MUT}$ tumors was as described previously (8). A KRAS gene signature was defined using a dataset of 84 lung adenocarcinomas (36), and subsequently validated with 2 independent cohorts of lung cancer (37,38) for which the KRAS mutation status was confirmed. Because the Shedden datasets were generated by 4 different laboratories, gene expression values within each subset were normalized to standard deviations from the mean. The Bhattacharjee KRAS signature consisted of "up" and "down" genes. Within each Shedden subset, the average of

"up" genes in the signature was compared with the average of "down" genes in the signature. Tumors with higher expression of the "up" or “down” genes ($p < 0.01$, t-test) were classified as positive or negative for the KRAS signature. The signature identified 143 tumors as KRAS signature$^{+/pos}$ and 116 tumors as wild-type or KRAS signature$^{-/neg}$ from 442 lung cancer patients (8). The remaining tumors were excluded from subsequent analyses. Within the KRAS signature subgroups, tumors were defined as having high or low expression of LAMB3, LAMA3, or LAMC2 if mRNA levels were higher or lower, respectively, than the median for that subset. Survival was estimated using the Kaplan-Meier method and P values were calculated with the log-rank (Mantel-Cox) test. Microarray data and clinical information on the Shedden samples (27) are available at https://array.nci.nih.gov/caarray/project/jacob-00182

RESULTS

A High-Throughput Screen of a Human miRNA Mimic Library Identifies Multiple miRNAs with Synthetic Lethality for Oncogenic KRAS

To identify human miRNAs that are synthetic lethal in cancer cells harboring oncogenic KRAS, we took advantage of an isogenic pair of HCT116 colon carcinoma cell lines expressing either wild-type KRAS (KRAS^{WT}) or an oncogenic mutant KRAS (KRAS^{MUT}, in this case KRAS^{G13D}). These cell lines were kindly provided by Dr. Bert Vogelstein laboratory. These cells were confirmed to show differential sensitivity to siRNA-mediated KRAS silencing (Figures S1A and S1B). We performed a high-throughput arrayed screen of a human miRNA mimic library (~858 mimics) to identify miRNAs that selectively kill cells carrying mutant KRAS (Figure 1A). miRNA mimics are designed to recapitulate the function of endogenous miRNAs but can also be modified to improve uptake and stability. Viability of HCT116 cells was measured with an ATP-based assay 5 days after library transfection, and three miRNA mimics were identified with selective lethality against HCT116 KRAS^{G13D} cells: hsa-miR-618, hsa-miR-1298, and hsa-miR-512-5p (Figure 1B). The two selection criteria were that the miRNA mimic had little or no effect on the viability of KRAS^{WT} cells (a viability score of 0.5–1.0, in which 1.0 indicates no effect) and had a significantly greater effect on the viability score of KRAS^{MUT} cells than on KRAS^{WT} cells (≥3-fold). The three hits identified in the screen were validated in more detailed assays using an independent fluorescence-based cell proliferation assay (Figure 1C). These experiments confirmed the specific and prolonged effects of miR-618, miR-1298, and miR-512-5p mimics on the viability of KRAS^{MUT} HCT116 cells.

miR-1298 is Selectively Lethal to Cells Expressing Oncogenic KRAS

We next asked whether the miRNA mimics identified in the HCT116 screen were also lethal in other KRAS mutant cell lines, and if so, whether they showed specificity for particular KRAS mutants. For this, we examined a panel of 9 NSCLC lines; 4 carrying KRAS^{WT} (H1568, H1437, H522, H520) and five harboring KRAS mutations (G12C: H23, H358, H1792; G12S: A549, and Q61H: H460). All lines express wild-type EGFR (Figure 2S). Among the three miRNA mimics tested, miR-1298 showed selective lethality on all of the KRAS^{MUT} cell lines, whereas the effects of miR-618 and miR-512-5p varied with the cell line (Figure 2A). RT-qPCR analysis showed miR-1298 expression was lower in KRAS

mutant NSCLC cell lines relative to cell lines with wild-type KRAS. (Figure S3A). Based on these results, we selected miR-1298 for further analysis.

The functional role of miR-1298 was assessed by examining colony formation in vitro and tumor growth in vivo. We found that the miR-1298 mimic inhibited foci formation by H460 ($KRAS^{MUT}$) cells but not by $KRAS^{WT}$ H1437 cells (Figure 2B), and significant H460 cell death by apoptosis was confirmed by TUNEL staining (Figure 2C and 4S). To determine the effect on tumor growth in vivo, miR-1298 or a control miRNA was overexpressed in $KRAS^{Q61H}$ and $KRAS^{G12S}$ cell lines (H460 and A549, respectively) using a lentiviral vector and transduced cells were injected subcutaneously into Balb/c nude mice. Tumor growth was then followed for up to 6 weeks. As was observed for in vitro growth, tumors derived from expressing miR-1298 cells grew at significantly slower rates than tumors expressing a control miRNA (Figure 2D). Thus, miR-1298 impairs the growth of oncogenic KRAS-driven cells both in vitro and in vivo.

miR-TRAP Technology Identifies LAMB3, FAK, PKP4, and WWP1 as miR-1298 Targets

miRNAs function by binding to their specific target mRNAs and promoting their degradation or inhibiting their translation. We took a two-pronged approach to identify putative downstream targets of miR-1298. First, we performed microarray analysis to identify differentially expressed genes in HCT116 cells transfected with miR-Ctrl or miR-1298. We then compared the most downregulated genes from the microarray analysis with the results of searches on rna22 (24) or TargetScan (http://www.targetscan.org); these programs use pattern-based predictive algorithms to identify potential miRNA target sites. From these two screens, the top 50 overlapping genes were chosen for further validation (Figure 3A).

To demonstrate direct interactions between miR-1298 and its target mRNAs in vivo, we turned to a recently reported method miR-TRAP (miRNA target RNA affinity purification) (25). For this, psoralen, a highly photoreactive probe, was conjugated to the 2′ position of the sugar ring of an amine-modified uridine residue 3′ of the miR-1298 seed sequence, and biotin was conjugated to the 3′ end for affinity purification (Figure 3B). The miR-1298-TRAP probe was transfected into HCT116 cells, and the cells were exposed to UVA (360 nm) to crosslink miR-1298-TRAP to its complementary mRNA. The miRNA–mRNA complexes were then affinity purified from cell lysates, and the isolated RNA was analyzed by RT-qPCR, using primers specific for the 50 genes described above (Figures 3B and S5). Using this relatively high-throughput assay, we identified 4 mRNAs among the 50 examined that showed significant enrichment in miR-1298-TRAP complexes from UVA-crosslinked cells compared with non-irradiated, but otherwise identically treated, cells. These mRNAs were *FAK* (focal adhesion kinase), *LAMB3* (laminin β3 subunit), *PKP4* (plakophilin-4), and *WWP1* (E3 ubiquitin ligase) (Figure 3C).

miR-1298 Functions Through FAK and LAMB3 Target mRNAs

To determine whether one or more of the four miR-1298 targets contributed to the synthetic lethality of miR-1298 in $KRAS^{MUT}$ cell lines, we knocked down FAK, LAMB3, PKP4, and WWP1 using SMARTpool siRNAs. Downregulation of both FAK and LAMB3 impaired the

viability of $KRAS^{MUT}$ cells, whereas knockdown of WWP1 and PKP4 was without effect (Figure 4A). PLK1 (8) and GATA2 (9) were also examined because both have been identified to have synthetic lethal interactions with oncogenic KRAS in NSCLC, which we confirmed here (Figure 4A). To rule out possible off-target effects of the LAMB3 and FAK siRNAs, we tested four siRNAs against each gene, and found that three of the four siRNAs effectively killed $KRAS^{MUT}$ cells (Figure S6A)

Importantly, the cytotoxic effects of siFAK and siLAMB3 on $KRAS^{MUT}$ lines correlated strongly with the effects of miR-1298 mimic (Figures 4B and 4C), consistent with FAK and LAMB3 being effectors of miR-1298 in these cells. Moreover, the FAK dependence of $KRAS^{MUT}$ cell lines was confirmed by treatment with a small molecule inhibitor of FAK, PF573228 (now VS-6063), which potently reduced $KRAS^{MUT}$ cell viability (Figure 4D).

To confirm that miR-1298 regulates the expression of FAK and LAMB3, we first examined their mRNA levels in miRNA-transfected cells. Indeed, both FAK and LAMB3 mRNA levels were significantly and selectively decreased in $KRAS^{MUT}$ cell lines by miR-1298 (Figures S6C and S6D). Next, using predictive algorithms, we determined the putative miR-1298 binding sites on FAK and LAMB3 mRNA using TargetScan and rna22, respectively. Based on the sequences predicted, we cloned the full length 3′UTR region of FAK and the miRNA response element (MRE) (26) in the coding region of LAMB3 into the psiCHECK2 luciferase reporter plasmid, upstream of the *Renilla* luciferase gene (Figure S6E). HeLa cells co-transfected with the LAMB3 or FAK reporter plasmid together with the miR-1298 mimic showed specific reductions in the ratio of *Renilla* luciferase to the constitutively expressed firefly luciferase, indicating that miR-1298 specifically recognizes, binds, and directs the degradation of both targets (Figure S6F). miR-1298 recognition and cleavage was confirmed to be sequence specific by demonstrating that mutants of these targeted sequences rescued *Renilla* luciferase activity (Figure S6F).

Finally, we asked whether overexpression of FAK and/or LAMB3 could prevent death of $KRAS^{MUT}$ lines induced by the miR-1298 mimic. Interestingly, the viability of miR-1298 mimic-transfected $KRAS^{MUT}$ lines was not significantly affected by overexpression of either LAMB3 or FAK alone, but co-expression of both proteins fully rescued the lethal effects of miR-1298 in multiple $KRAS^{MUT}$ lines (Figure 5A). These results demonstrate that, although knockdown of either gene mimics the effect of miR-1298, both proteins are necessary to prevent miR-1298-induced death.

LAMB3 is Transcriptionally Regulated by mutant KRAS

To determine how LAMB3 and FAK intersect with the oncogenic KRAS pathway, we examined their mRNA and protein expression after knocking down KRAS in $KRAS^{MUT}$ lines and overexpressing $KRAS^{G12V}$ in $KRAS^{WT}$ cells. Interestingly, LAMB3 mRNA levels were markedly reduced by siKRAS treatment of $KRAS^{MUT}$ lines (Figure 5B) and dramatically increased in $KRAS^{WT}$ cells overexpressing oncogenic $KRAS^{G12V}$ (Figure 5D). LAMB3 protein expression was similarly affected (Figures 5C and 5E). Surprisingly, expression of FAK mRNA (Figure S7) and protein (Figures 5C and 5E) was entirely unaffected by the same treatments. We also found that knockdown and overexpression of mutant KRAS similarly did not affect the expression of miR-1298 (Figure S3B and S3C).

These findings suggest that LAMB3 is a downstream transcriptional target of KRAS, but that miR-1298 and FAK are not directly affected. On the other hand, FAK does not appear to have direct interactions within the KRAS pathway but mutant KRAS cells are highly sensitized to changes in FAK expression. This highlights the utility of unbiased functional synthetic lethal genomic screens in identifying interactions that could not be predicted based on differential expression.

LAMB3 Expression Predicts Survival Probability of NSCLC Patients with Oncogenic KRAS

To determine the clinical significance of our observations, we analyzed gene expression data from a cohort of 259 lung cancer patients for whom the survival outcome and KRAS transcriptional signature status are known (27). The 143 KRAS signature^{pos} patients and 116 KRAS signature^{neg} patients were stratified according to LAMB3 and FAK mRNA expression, with high and low expression classified as greater than or less than the median expression levels, respectively. Survival outcome was then analyzed using a previously established method (8). Interestingly, high LAMB3 expression was significantly associated with poorer overall survival of patients harboring KRAS signature^{pos} tumors but not those with KRAS signature^{neg} tumors (Figure 6A), whereas *FAK* expression was without prognostic value (Figure 6B), which was also seen in another study of prognosis in early stage NSCLC (28). Finally, because *LAMB3* is one subunit of the laminin 332 heterotrimer, we also examined the possible involvement of the remaining subunits, LAMA3 and LAMC2. Interestingly, siRNA-mediated knockdown of either protein had no effect on the viability of KRAS^{WT} or KRAS^{MUT} cell lines (Figure S8A) and there was no detectable correlation between expression of *LAMA3* or *LAMC2* and the prognosis of patients with KRAS gene signature^{pos} NSCLC (Figure S8B). Collectively, these findings suggest that differences in *LAMB3* expression are clinically relevant in KRAS^{MUT} lung cancers, and thus LAMB3 may be useful not only as a potential therapeutic target but also as a prognostic biomarker. In contrast to LAMB3, FAK expression is not affected by mutant KRAS. As such, the clinical outcome in KRAS signature^{pos} NSCLC is LAMB3 dependent but not FAK dependent.

DISCUSSION

KRAS mutant cancers are among the most difficult to treat with poor survival and resistance to chemotherapy and newer targeted therapies and agents to target KRAS mutant cancers remain an unmet clinical need in CRC and NSCLC. In this study, we performed a large-scale synthetic lethal screen in an isogenic CRC cell line pair to identify miRNAs that are selectively lethal for KRAS^{MUT} cells and confirmed these miRNAs in a panel of cell lines harboring different oncogenic KRAS mutations, and then used miR-TRAP approach to identify functional miRNA targets. Collectively, these experiments identified miR-1298 and its downstream targets LAMB3 and FAK as a potentially targetable regulatory axis in KRAS mutated tumor cells (Figure 6C). Furthermore, the clinical relevance of these findings was revealed by demonstrating a significant correlation between *LAMB3* expression and survival specifically in lung cancer patients positive for a KRAS gene expression signature.

LAMA3, LAMB3, and *LAMC2* encode the of α3, β2, and γ2 subunits, respectively, of the trimeric basement membrane protein laminin 332 (29). Laminin 332 has been shown to promote tumorigenesis in squamous cell carcinoma through interactions with cell surface receptors such as integrins, epidermal growth factor receptor, and syndecan 1 (29,30). In addition, human squamous cell carcinoma induced by $HRAS^{V12}$ and IκBα can be inhibited by blocking antibodies against laminin 332 or β4 integrins (31). In models of human epidermal carcinogenesis, LAMB3 activates PI3K through interactions with collagen VII (32). LAMB3 was also identified in a large siRNA synthetic lethal screen in similar isogenic KRAS CRC cell lines (11) further validating our synthetic lethal miRNA screen. We also demonstrated that LAMB3 expression is affected by KRAS oncogenic mutations and LAMB3 expression level correlated with survival. The association between KRAS mutations and LAMB3 expression raises the possibility of LAMB3 as a prognostic biomarker in KRAS mutated NSCLC. Given our results, LAMB3 also may serve as a biomarker to identify patients in whom targeting the miR-1298/FAK/LAMB3 axis might have clinical benefit.

The second specific miR-1298 target mRNA we identified is FAK (PTK2), a tyrosine kinase component of focal adhesion complexes that has been implicated as a crucial mediator at the intersection of many different signaling pathways with diverse effects in cancer including promoting tumor progression and metastasis, the maintenance of cancer stem cells, and modulation the tumor microenvironment and angiogenesis (33). Binding and phosphorylation of FAK tyrosine 925 by Src family kinases creates a Grb2 SH2-domain binding site and provides a link to activation of the RAS signal transduction pathway (34). Furthermore, previous studies have shown that RhoA–FAK signaling is required for maintenance of KRAS-driven adenocarcinomas (35), and Defactinib (VS-6063) a FAK small molecule inhibitor is currently in phase II clinical trial in KRAS mutant NSCLC. Our data highlight the significance of FAK not just in RhoA signaling, but implicates FAK in oncogenic KRAS-driven cancers and suggests that FAK small molecule inhibitors may be used to treat KRAS-driven cancers more generally than previously envisioned. Given the current complexity in terms of diverse mechanisms in FAK on human cancers, our finding of a novel regulatory axis through miR-1298 on the expression of FAK and LAMB3 as a potential vulnerability in KRAS driven cancers suggests future mechanistic studies focusing on the interaction of integrins with FAK and RAS signaling may provide further insight towards targeting this signaling axis. Also, given the frequent use of anti-angiogenesis therapies in NSCLC and CRC, future studies on the association between FAK and angiogenesis may also provide further insight into potential novel therapies for KRAS mutated cancers.

In summary, our study has revealed a novel role for miR-1298 in the survival of $KRAS^{MUT}$ tumor cells and identified two target genes, LAMB3 and FAK, with potential therapeutic value for KRAS-driven cancers. Our work emphasizes the utility of miRNAs as tools with which to probe complex biological processes and to identify novel therapeutic targets.

Supplementary Material

Refer to Web version on PubMed Central for supplementary material.

Acknowledgments

We are grateful to Dr. Bert Vogelstein for HCT116 and RasWT1 (HAF1) cell lines; Dr. Baigude for help in miR-TRAP experiments, Dr. Peter Marinkovich for laminin antibodies; Chad J. Creighton, Ji Luo, and Stephen J. Elledge for sharing the KRAS signature genes, and David G. Beer, Kevin K. Dobbin, and Guoan Chen for their generous assistance in mapping the sample IDs of the Shedden dataset.

Reference

1. Berndt N, Hamilton AD, Sebti SM. Targeting protein prenylation for cancer therapy. Nat Rev Cancer. 2011; 11(11):775–791. [PubMed: 22020205]
2. Knickelbein K, Zhang L. Mutant KRAS as a critical determinant of the therapeutic response of colorectal cancer. Genes Dis. 2015; 2(1):4–12. [PubMed: 25815366]
3. Arkin MR, Wells JA. Small-molecule inhibitors of protein-protein interactions: progressing towards the dream. Nature reviews Drug discovery. 2004; 3(4):301–317. [PubMed: 15060526]
4. Sun Q, Burke JP, Phan J, Burns MC, Olejniczak ET, Waterson AG, et al. Discovery of Small Molecules that Bind to K-Ras and Inhibit Sos-Mediated Activation. Angewandte Chemie International Edition. 2012; 51(25):6140–6143. [PubMed: 22566140]
5. Zimmermann G, Papke B, Ismail S, Vartak N, Chandra A, Hoffmann M, et al. Small molecule inhibition of the KRAS-PDE[dgr] interaction impairs oncogenic KRAS signalling. Nature. 2013 advance online publication.
6. Shima F, Yoshikawa Y, Ye M, Araki M, Matsumoto S, Liao J, et al. In silico discovery of small-molecule Ras inhibitors that display antitumor activity by blocking the Ras–effector interaction. Proceedings of the National Academy of Sciences. 2013; 110(20):8182–8187.
7. Barbie DA, Tamayo P, Boehm JS, Kim SY, Moody SE, Dunn IF, et al. Systematic RNA interference reveals that oncogenic KRAS-driven cancers require TBK1. Nature. 2009; 462(7269):108–112. [PubMed: 19847166]
8. Luo J, Emanuele MJ, Li D, Creighton CJ, Schlabach MR, Westbrook TF, et al. A Genome-wide RNAi Screen Identifies Multiple Synthetic Lethal Interactions with the Ras Oncogene. Cell. 2009; 137(5):835–848. [PubMed: 19490893]
9. Kumar Madhu S, Hancock David C, Molina-Arcas M, Steckel M, East P, Diefenbacher M, et al. The GATA2 Transcriptional Network Is Requisite for RAS Oncogene-Driven Non-Small Cell Lung Cancer. Cell. 2012; 149(3):642–655. [PubMed: 22541434]
10. Scholl C, Fröhling S, Dunn IF, Schinzel AC, Barbie DA, Kim SY, et al. Synthetic Lethal Interaction between Oncogenic KRAS Dependency and STK33 Suppression in Human Cancer Cells. Cell. 2009; 137(5):821–834. [PubMed: 19490892]
11. Steckel M, Molina-Arcas M, Weigelt B, Marani M, Warne PH, Kuznetsov H, et al. Determination of synthetic lethal interactions in KRAS oncogene-dependent cancer cells reveals novel therapeutic targeting strategies. Cell Res. 2012; 22(8):1227–1245. [PubMed: 22613949]
12. Shaw AT, Winslow MM, Magendantz M, Ouyang C, Dowdle J, Subramanian A, et al. Selective killing of K-ras mutant cancer cells by small molecule inducers of oxidative stress. Proceedings of the National Academy of Sciences. 2011; 108(21):8773–8778.
13. Iyer MK, Niknafs YS, Malik R, Singhal U, Sahu A, Hosono Y, et al. The landscape of long noncoding RNAs in the human transcriptome. Nat Genet. 2015; 47(3):199–208. [PubMed: 25599403]
14. Pritchard CC, Cheng HH, Tewari M. MicroRNA profiling: approaches and considerations. Nature reviews Genetics. 2012; 13(5):358–369.
15. Ebert Margaret S, Sharp Phillip A. Roles for MicroRNAs in Conferring Robustness to Biological Processes. Cell. 2012; 149(3):515–524. [PubMed: 22541426]
16. Lu J, Getz G, Miska EA, Alvarez-Saavedra E, Lamb J, Peck D, et al. MicroRNA expression profiles classify human cancers. Nature. 2005; 435(7043):834–838. [PubMed: 15944708]
17. Kumar MS, Lu J, Mercer KL, Golub TR, Jacks T. Impaired microRNA processing enhances cellular transformation and tumorigenesis. Nat Genet. 2007; 39(5):673–677. [PubMed: 17401365]

18. Johnson SM, Grosshans H, Shingara J, Byrom M, Jarvis R, Cheng A, et al. RAS Is Regulated by the let-7 MicroRNA Family. Cell. 2005; 120(5):635–647. [PubMed: 15766527]
19. Johnson CD, Esquela-Kerscher A, Stefani G, Byrom M, Kelnar K, Ovcharenko D, et al. The let-7 MicroRNA Represses Cell Proliferation Pathways in Human Cells. Cancer Research. 2007; 67(16):7713–7722. [PubMed: 17699775]
20. Kumar MS, Erkeland SJ, Pester RE, Chen CY, Ebert MS, Sharp PA, et al. Suppression of non-small cell lung tumor development by the let-7 microRNA family. Proceedings of the National Academy of Sciences. 2008; 105(10):3903–3908.
21. Yu S, Lu Z, Liu C, Meng Y, Ma Y, Zhao W, et al. miRNA-96 suppresses KRAS and functions as a tumor suppressor gene in pancreatic cancer. Cancer Res. 2010; 70(14):6015–6025. [PubMed: 20610624]
22. Shin KH, Bae SD, Hong HS, Kim RH, Kang MK, Park NH. miR-181a shows tumor suppressive effect against oral squamous cell carcinoma cells by downregulating K-ras. Biochem Biophys Res Commun. 2011; 404(4):896–902. [PubMed: 21167132]
23. Liao WT, Ye YP, Zhang NJ, Li TT, Wang SY, Cui YM, et al. MicroRNA-30b functions as a tumour suppressor in human colorectal cancer by targeting KRAS, PIK3CD and BCL2. J Pathol. 2014; 232(4):415–427. [PubMed: 24293274]
24. Miranda KC, Huynh T, Tay Y, Ang Y-S, Tam W-L, Thomson AM, et al. A Pattern-Based Method for the Identification of MicroRNA Binding Sites and Their Corresponding Heteroduplexes. Cell. 2006; 126(6):1203–1217. [PubMed: 16990141]
25. Baigude H, Ahsanullah, Li Z, Zhou Y, Rana TM. miR-TRAP: A Benchtop Chemical Biology Strategy to Identify microRNA Targets. Angewandte Chemie International Edition. 2012; 51(24): 5880–5883. [PubMed: 22566243]
26. Tay Y, Zhang J, Thomson AM, Lim B, Rigoutsos I. MicroRNAs to Nanog, Oct4 and Sox2 coding regions modulate embryonic stem cell differentiation. Nature. 2008; 455(7216):1124–1128. [PubMed: 18806776]
27. Shedden K, Taylor JM, Enkemann SA, Tsao MS, Yeatman TJ, Gerald WL, et al. Gene expression-based survival prediction in lung adenocarcinoma: a multi-site, blinded validation study. Nature medicine. 2008; 14(8):822–827.
28. Dy GK, Ylagan L, Pkharel S, Miller A, Brese E, Bshara W, Morrison C, Cance WG, Golubovskaya VM. The prognostic significance of focal adhesion kinase expression in stage I non-small-cell lung cancer. J Thorac Oncol. 2014; 9(9):1278–1284. [PubMed: 25122425]
29. Marinkovich MP. Laminin 332 in squamous-cell carcinoma. Nat Rev Cancer. 2007; 7(5):370–380. [PubMed: 17457303]
30. Ortiz-Urda S, Garcia J, Green CL, Chen L, Lin Q, Veitch DP, et al. Type VII Collagen Is Required for Ras-Driven Human Epidermal Tumorigenesis. Science. 2005; 307(5716):1773–1776. [PubMed: 15774758]
31. Dajee M, Lazarov M, Zhang JY, Cai T, Green CL, Russell AJ, et al. NF-[kappa]B blockade and oncogenic Ras trigger invasive human epidermal neoplasia. Nature. 2003; 421(6923):639–643. [PubMed: 12571598]
32. Waterman EA, Sakai N, Nguyen NT, Horst BAJ, Veitch DP, Dey CN, et al. A Laminin-Collagen Complex Drives Human Epidermal Carcinogenesis through Phosphoinositol-3-Kinase Activation. Cancer Research. 2007; 67(9):4264–4270. [PubMed: 17483338]
33. Sulzmaier FJ, Jean C, Schlaepfer DD. FAK in cancer: mechanistic findings and clinical applications. Nat Rev Cancer. 2014; 14(9):598–610. [PubMed: 25098269]
34. Schlaepfer DD, Hanks SK, Hunter T, Geer Pvd. Integrin-mediated signal transduction linked to Ras pathway by GRB2 binding to focal adhesion kinase. Nature. 1994; 372(6508):786–791. [PubMed: 7997267]
35. Konstantinidou G, Ramadori G, Torti F, Kangasniemi K, Ramirez RE, Cai Y, et al. RHOA-FAK is a required signaling axis for the maintenance of KRAS-driven adenocarcinomas. Cancer Discovery. 2013
36. Bhattacharjee A, Richards WG, Staunton J, Li C, Monti S, Vasa P, et al. Classification of human lung carcinomas by mRNA expression profiling reveals distinct adenocarcinoma subclasses.

Proceedings of the National Academy of Sciences of the United States of America. 2001; 98(24): 13790–13795. [PubMed: 11707567]

37. Beer DG, Kardia SL, Huang CC, Giordano TJ, Levin AM, Misek DE, et al. Gene-expression profiles predict survival of patients with lung adenocarcinoma. Nature medicine. 2002; 8(8):816–824.

38. Ding L, Getz G, Wheeler DA, Mardis ER, McLellan MD, Cibulskis K, et al. Somatic mutations affect key pathways in lung adenocarcinoma. Nature. 2008; 455(7216):1069–1075. [PubMed: 18948947]

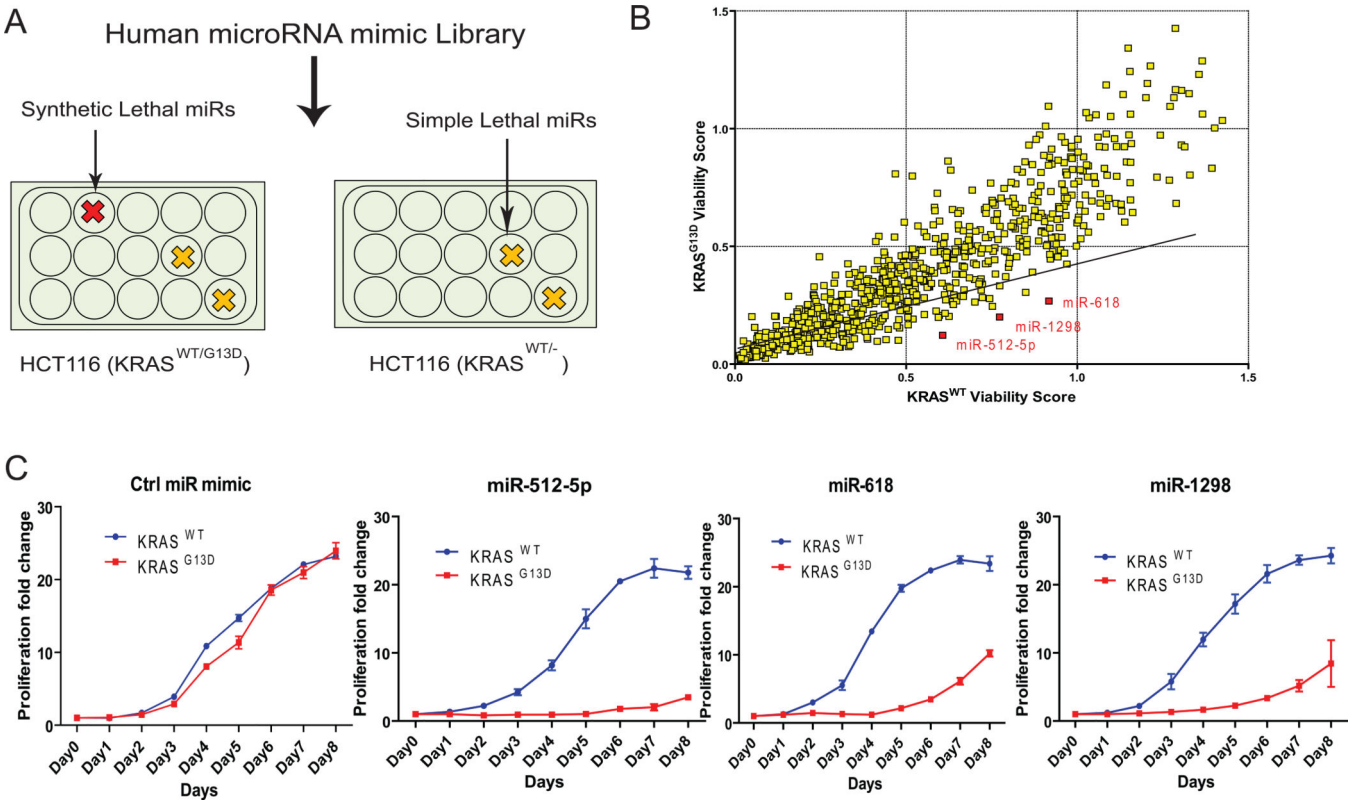

Figure 1. Functional Genomics Screening of a Human miRNA Mimic Library in an Isogenic Pair of HCT116 Cells

(A) Schematic showing method of hit selection from the synthetic lethal screen.

(B) Results of the screen of a human miRNA mimic library (~858 mimics, Ambion). HTC116 cell were reverse transfected and viability was determined 5 days later. Viability scores are the averages of triplicate wells normalized to cells treated with control miRNA mimic. miRNA mimics were considered hits (red squares) if they reduced the viability score of HCT116 $KRAS^{G13D}$ cells by at least 3-fold compared with HCT116 $KRAS^{WT}$, and the viability score of $KRAS^{WT}$ cells was ≥0.7.

(C) Secondary validation of hits from (B) in an independent assay of HCT116 cell proliferation (CyQUANT). Results are the mean ± standard deviation of n = 3.

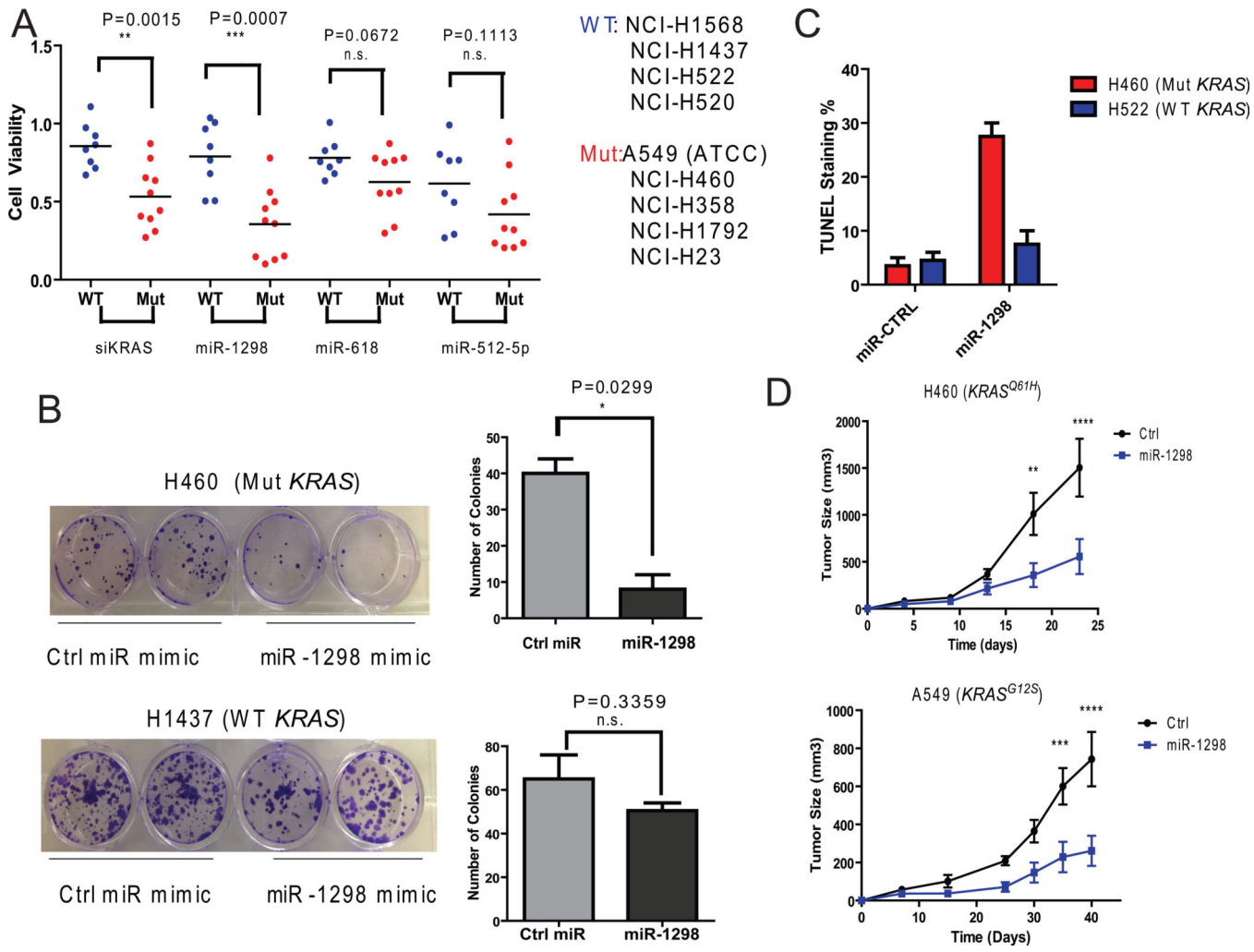

Figure 2. miR-1298 Mimic Selectively Kills NSCLC Lines Harboring Mutant KRAS and Inhibits Colony Formation In Vitro and Tumor Formation In Vivo

(A) Viability of NSCLC lines expressing $KRAS^{WT}$ (4 cell lines; blue) or $KRAS^{MUT}$ (5 cell lines; red) 5 days after transfection with the indicated miRNA mimics or siRNA. Dots indicate duplicates of each cell line. Statistical analysis by unpaired t-test.

(B) Colony formation by H460 ($KRAS^{Q61H}$) or H1437 ($KRAS^{WT}$) 2 weeks after transfection with control or miR-1298 mimics. Results are the mean ± standard deviation of n = 3. Statistical analysis by two-tailed Student's t-test.

(C) Quantification of $TUNEL^{+}$ H460 ($KRAS^{Q61H}$) and H522 ($KRAS^{WT}$) cells 5 days after transfection with miRNA mimics. Results are the mean standard deviation of n = 3.

(D) Tumor formation in Balb/c nude mice injected subcutaneously with H460 ($KRAS^{Q61H}$) or A549 ($KRAS^{G12S}$) cells infected with miR-1298 or miR-Ctrl lentiviruses. Results are the mean ± standard deviation of 6 mice per group. **p < 0.01, ***p < 0.001, ****p < 0.0001 by two-way repeated measures ANOVA with Bonferroni's post hoc test.

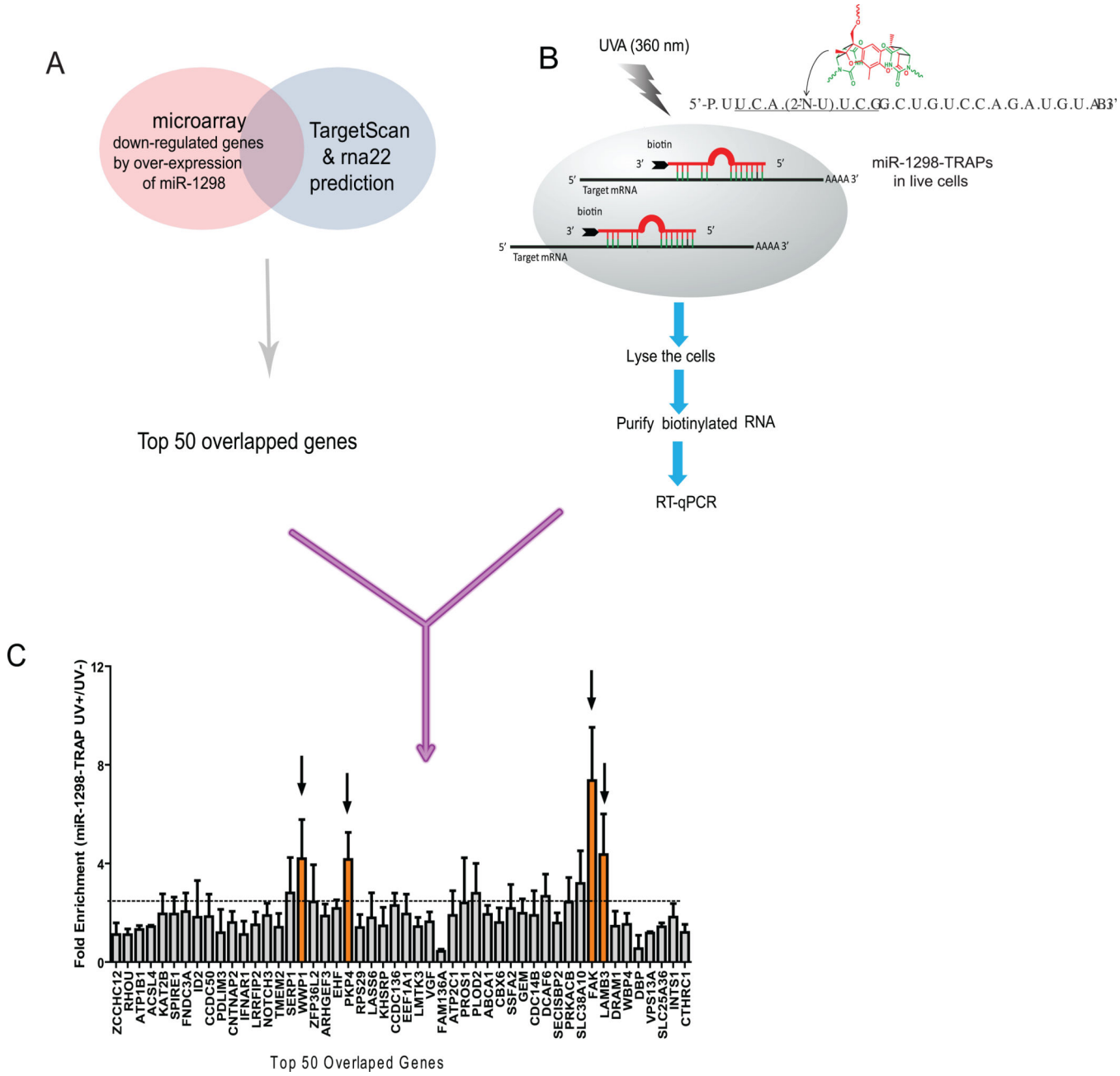

Figure 3. Target Validation of miR-1298 Using miR-TRAP Technology

(A) Selection of miR-1298 potential targets. The top 50 candidate genes were chosen by comparing genes selectively downregulated by overexpression of miR-1298 with putative miRNA targets generated by the rna22 and TargetScan predictive algorithms.

(B) Schematic of the miR-TRAP method. HCT116 cells expressing biotinylated and psoralen-modified miR-1298-TRAP were UVA-irradiated to crosslink miRNA mimics with target mRNA, or remained non-irradiated (controls). miRNA mimics were affinity purified and associated RNA was analyzed by RT-qPCR.

(C) RT-qPCR analysis of the 50 candidate genes in samples of RNA isolated from the miR-TRAP experiment shown in (B). Results are expressed as the fold enrichment in samples

isolated from irradiated vs. non-irradiated miR-1298-TRAP-expressing cells. Four genes showed specific enrichment: WWP1, PKP4, FAK, and LAMB3. Mean standard deviation of n = 3.

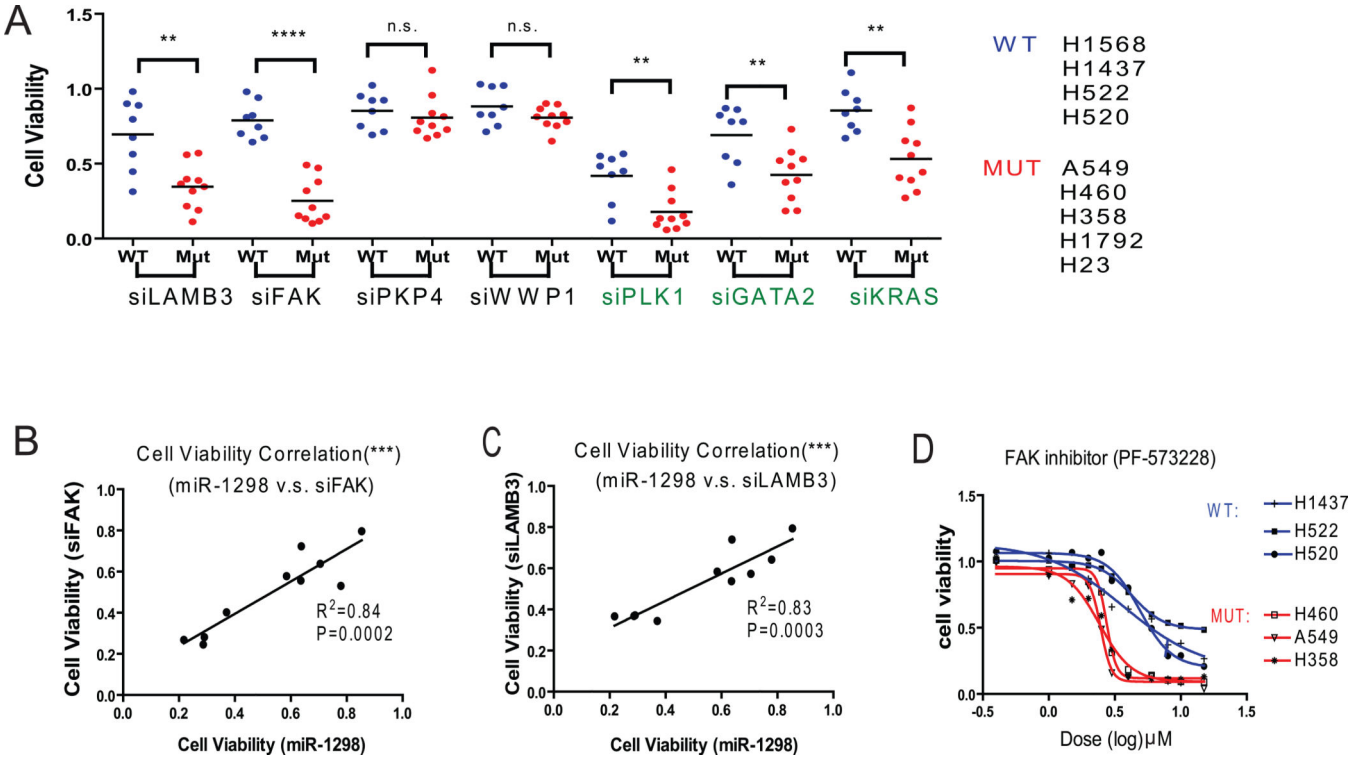

Figure 4. miR-1298 Functional Targets FAK and LAMB3 are Required for Growth of NSCLC Cells Harboring Mutant KRAS

(A) Viability of $KRAS^{WT}$ (blue) or $KRAS^{MUT}$ (red) NSCLC cells 4 days after transfection with SMARTpool siRNAs targeting the putative miR-1298 targets FAK, LAMB3, WWP1, and PKP4, or positive control proteins PLK1, GATA2, and KRAS. Each line was tested in duplicate. **p < 0.01, ****p < 0.0001 by unpaired t-test.

(B–C) Correlation between effects of miR-1298 mimic and siFAK (B) or siLAMB3 (C) on viability of NSCLC ($KRAS^{MUT}$) lines.

(D) Viability of NSCLC lines incubated with the indicated concentrations of the FAK inhibitor (PF-573228).

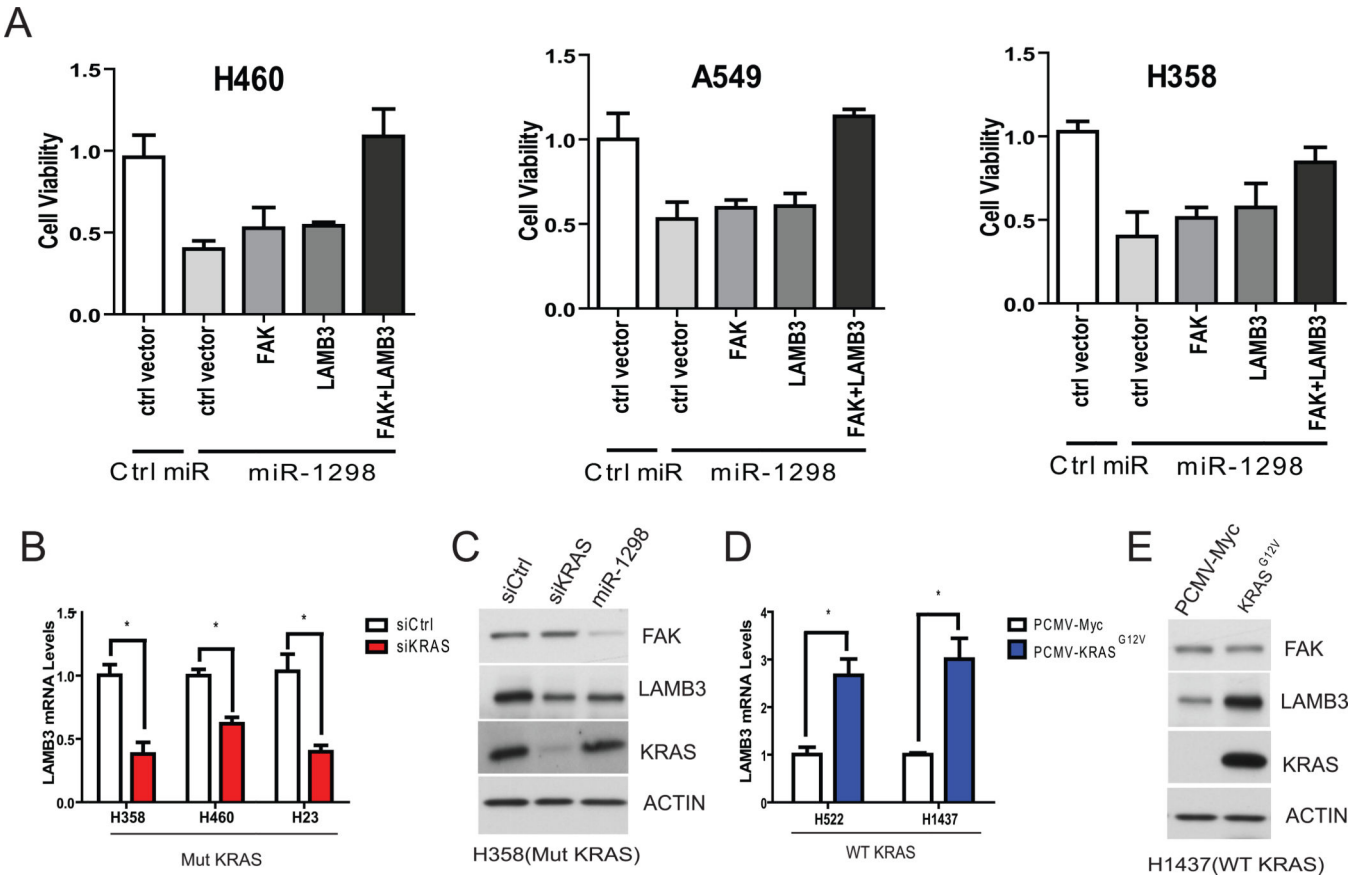

Figure 5. Overexpression of FAK and LAMB3 Inhibits Death of KRAS^{WT} NSCLC Lines Induced by miR-1298

(A) Viability of KRAS^{MUT} NSCLC lines after transfection with the indicated combinations of miR-1298 or miR-Ctrl mimics and FAK and LAMB3 overexpression plasmids. Results are the mean ± standard deviation of n = 3.

(B) RT-qPCR analysis of LAMB3 mRNA levels in KRAS^{MUT} NSCLC lines after transfection with KRAS or control siRNA.

(C) Immunoblot analysis of FAK, LAMB3, KRAS, and actin in H358 (KRAS^{MUT}) cells after transfection with the indicated siRNA or miRNA mimic.

(D) RT-qPCR analysis of LAMB3 mRNA in KRAS^{WT} NSCLC cells after transfection with control or KRAS^{G12V} expression vectors.

(E) Immunoblot analysis of FAK, LAMB3, KRAS, and actin in H1437 (KRAS^{WT}) cells after transfection with the indicated expression vectors. Results in B and D are the mean ± standard deviation of n = 3. *p < 0.05.

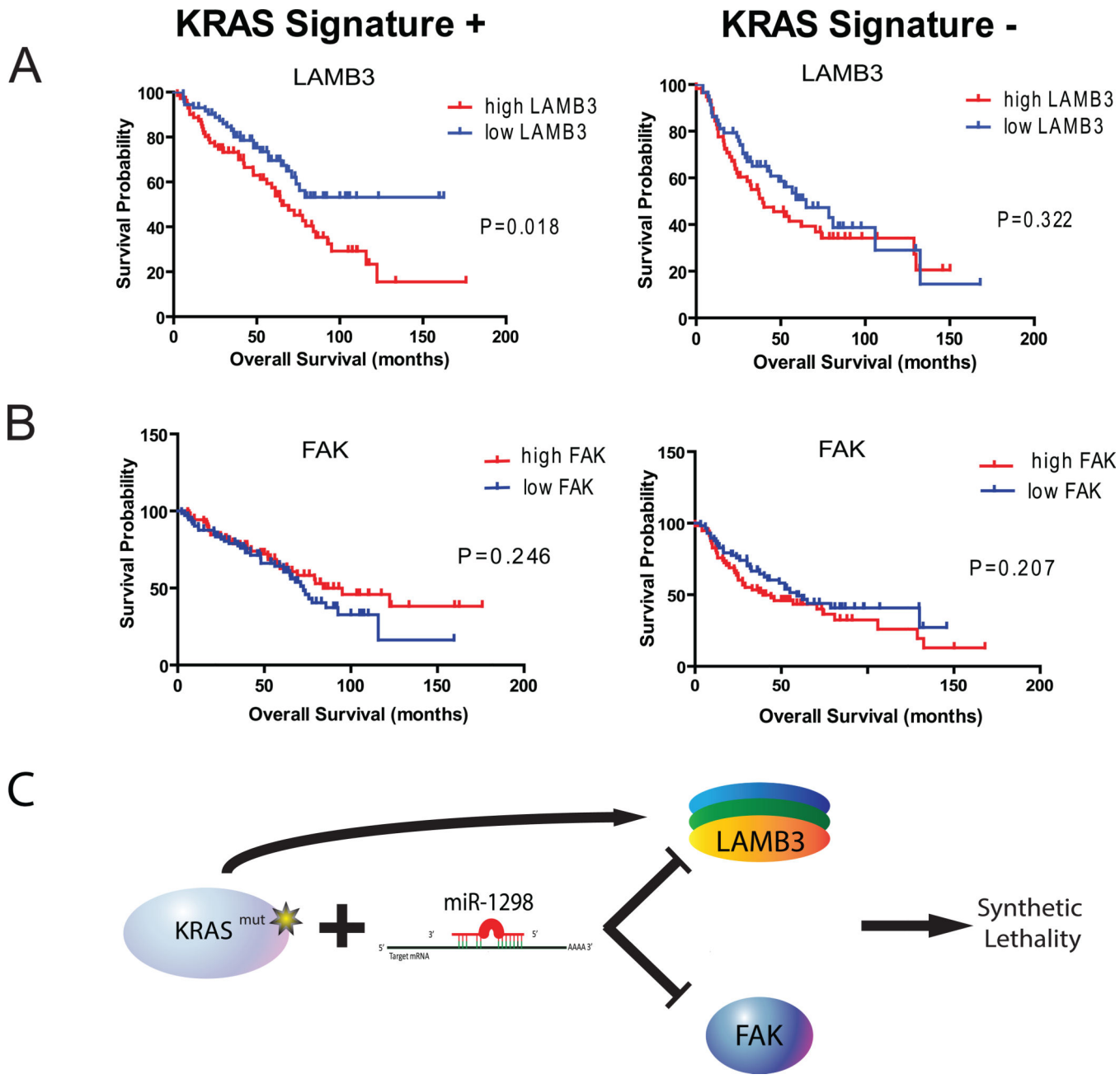

Figure 6. LAMB3 Expression Predicts Survival of NSCLC Patients with Tumors Expressing a KRAS Gene Signature

(A–B) Correlation of LAMB3 (A) and FAK (B) mRNA expression with overall survival of patients with tumors positive or negative for the KRAS signature (Kaplan-Meier analysis). Tumors were scored as having LAMB3 or FAK mRNA levels higher (red line) or lower (blue line) than the median level of expression. P values determined by log-rank (Mantel-Cox) test. N = 143 or 116 for patients with KRAS signature^{pos} and KRAS signature^{neg} tumors, respectively.

(C) Model of miR-1298-regulated synthetic lethality of $KRAS^{MUT}$ NSCLC through FAK and LAMB3.